Ecology and Evolution

Investigating sex-specific dynamics using uniparental markers: West New Guinea as a case study

Stefano Mona[1,2], Ernest Mordret[1,2], Michel Veuille[1,2] & Mila Tommaseo-Ponzetta[3]

[1]Laboratoire Biologie intégrative des populations, Ecole Pratique des Hautes Etudes, 46 rue de Lille, 75007 Paris, France
[2]CNRS UMR 7205, Muséum National d'Histoire Naturelle, Rue Buffon, 75005 Paris, France
[3]Department of Biology, University of Bari, 70100 Bari, Italy

Abstract

Mitochondrial DNA (mtDNA) and Y chromosome (NRY) genetic markers have been often contrasted to investigate sex-specific dynamics. Traditionally, isolation by distance, intrapopulation genetic diversity and population differentiation are estimated from both markers and compared. Two possible sources of bias are often neglected. First, kilometric distances are frequently used as predictor of the connectivity between groups, hiding the role played by environmental features at a microgeographic scale. Second, the comparison of intrapopulation diversity and population differentiation between mtDNA and NRY is hampered by their different mutational mechanisms and rates. Here, we show how to account for these biases by analyzing from a different perspective a published dataset of eight West New Guinea (WNG) populations for which mtDNA control region sequences and seven linked NRY microsatellites had been typed. First, we modeled the connectivity among sampled populations by computing the number of days required to travel between groups. Then, we investigated the differences between the two sexes accounting for the molecular characteristics of the markers examined to obtain estimates on the product of the effective population size and the migration rate among demes (Nm). We achieved this goal by studying the shape of the gene genealogy at several sampling levels and using spatial explicit simulations. Both the direction and the rate of migration differ between male and females, with an Nm estimated to be >6 times higher in the latter under many evolutionary scenarios. We finally highlight the importance of applying metapopulation models when analyzing the genetic diversity of a species.

Introduction

Sex-specific demographic patterns are traditionally investigated in humans by using uniparentally inherited markers, namely mitochondrial DNA (mtDNA) for females and Y chromosome (NRY) for males. Reports usually focus mainly on three classes of analysis, whose results are compared between the two markers: (i) isolation by distance (IBD) (Seielstad et al. 1998; Wood et al. 2005; Delfin et al. 2012; Kemp et al. 2012); (ii) intrapopulation diversity levels (Oota et al. 2001; Kayser et al. 2003; Gunnarsdottir et al. 2012); (iii) extent of population differentiation (Seielstad et al. 1998; Oota et al. 2001; Nasidze et al. 2004). Most of the evidences presented so far suggest that paternal and maternal histories differ heavily, probably

as a consequence of cultural behaviors related to postmarital residential pattern and variance in reproductive success (see Heyer et al. [2012] and references therein). However, different conclusions have been drawn depending on the region investigated (Seielstad et al. 1998; Oota et al. 2001; Fuselli et al. 2003; Kayser et al. 2003; Nasidze et al. 2004; Kemp et al. 2012), on the geographic scale of the study (Wilder et al. 2004; Wilkins and Marlowe 2006) and on the specific locus ascertained on both mtDNA and NRY (Wilder et al. 2004; Gunnarsdottir et al. 2012).

There are several pitfalls when investigating male and female population genetics patterns. First, despite the advances in next generation sequencing technologies which allow access to an incredibly large amount of data

(Metzker 2010), comparison of male and female population dynamics still relies on a small and nonrecombining portion of our genome (however, see Balaresque et al. 2006; Segurel et al. 2008 for exceptions). This limits the possibility of accounting for the large stochastic variance associated with the coalescent process, which can be mitigated through the analysis of as many independent loci as possible (Felsenstein 2006). Second, IBD analysis usually relies on simple kilometric distance matrices and does not take explicitly into account environmental features, which can affect connectivity among populations (McRae and Beier 2007). Third, population genetic models used often assume equilibrium (i.e., Wright [1931] island model), hence ignoring both temporal and spatial heterogeneity. Indeed, human societies have probably changed their lifestyle on multiple occasions. Moreover, the carrying capacity of various habitats has not been constant through time due, for instance, to technological innovations, leading to variation in the effective size of human populations. Fourth, mutation rate influences both the gene diversity of a sample (Hudson 1990) and many frequently used measure of population differentiation such as Fst and Rst (Hedrick 2005; Meirmans 2006). This must be acknowledged when comparing the results obtained from loci with different mutation rates such as mtDNA and NRY microsatellites.

In this report, we show how to cope with the differences among the markers to be compared and the advantages of taking environmental features into account when modeling genetic diversity. To this end, we analyzed in a new light a published dataset of mtDNA and NRY microsatellites variation in eight West New Guinea (WNG) groups (Tommaseo-Ponzetta et al. 2002; Kayser et al. 2003). The long human presence in the island as well as the environmental and temporal heterogeneity makes WNG an interesting region to investigate population dynamics and contrast male and female histories. New Guinea was colonized in the last part of the Pleistocene when the island, together with Australia and Tasmania, was part of one paleocontinent called "Sahul". Although the earliest human presence in the highlands of New Guinea is documented 49,000 years ago (Summerhayes et al. 2010), by analogy with Australian prehistoric evidence this occupation may have been even earlier (Roberts et al. 1990; Fullagar et al. 1996; O'Connell and Allen 1998; Thorne et al. 1999). The first migrants were hunter–gatherers who probably spread along the coast of the continent, leaving little evidence of their passage. Later, many hunter–gatherer groups in the highland plateaus shifted to agriculture. According to archaeological findings, an independent origin of agriculture in New Guinea can be dated as far back as 10,000–9000 years before present, with more intensive cultivation of various species starting

by 7000–6500 years before present in Papua New Guinea (Golson 1990; Denham et al. 2003; Denham 2005).

The analyzed populations cover two regions of WNG with different environmental characteristics: three of the eight groups are farmers, inhabiting the interior highlands, whereas the remaining five are hunter/fisher–gatherers (Tommaseo-Ponzetta et al. 2002), inhabiting the lowlands. A reduced NRY diversity compared with mtDNA was already put forward when analyzing these eight groups (Kayser et al. 2003), making them suitable for more in-depth comparison. The differences between the two sexes were mostly explained as a by-product of patrilocality and polygyny (Kayser et al. 2003) (recently, however, Heyer et al. [2012] showed that polygyny alone has a limited influence on male effective population size), but no formal hypothesis testing was carried out to obtain quantitative estimate on their intensities.

Here, we took environmental conditions into account by recording the walking time between the eight groups. Furthermore, we compared the demography of males and females using the prediction of the sampling theory in a metapopulation (Wakeley and Lessard 2003; De and Durrett 2007; Stadler et al. 2009). In particular, we investigated the shape of the gene genealogy within each population and in pooled samples to qualitatively estimate the product of effective population size and migration rate of the metapopulation (Nm). The shape of the genealogy does not depend on the neutral mutation rate (Wakeley 2008), therefore it is possible to perform an unbiased comparison of the Nm values of any markers. Finally, we performed spatially explicit simulations to investigate the population structure at both mtDNA and NRY, modeling their molecular evolution properties as well as the environmental and temporal heterogeneity (such as the emergence of agriculture) of WNG.

In agreement with patrilocality and polygyny, we found a strong difference between male and female dynamics in WNG, both in terms of direction and rate of gene flow. The pattern of those differences and their magnitude emerged when analyzing data under a metapopulation approach, both indirectly by investigating the shape of the gene genealogy and directly by simulations taking environmental conditions and locus-specific characteristics into account.

Material and Methods

Population samples

We included 200 mtDNA (Tommaseo-Ponzetta et al. 2002) and 163 NRY (Kayser et al. 2003) samples belonging to five populations of hunter/fisher gatherers (Asmat, Awyu, Citak, Mappi, Muyu) and three populations of

agriculturalists (Dani, Ketengban, Una). The hunter/fisher gatherers groups (HG) inhabit the southern lowlands of WNG whereas agriculturalists (AG) inhabit the central and western highlands (Fig. 1). More details on these populations are available elsewhere (Tommaseo-Ponzetta et al. 2002). We analyzed 350 bp of the hypervariable segment 1 of the mitochondrial control region (Tommaseo-Ponzetta et al. 2002; data available from GenBank) and seven NRY microsatellites, namely DYS19, DYS389I, DYS389II, DYS390, DYS391, DYS392, and DYS393 (Kayser et al. 2003, data available upon request). We did not use NRY haplogroup frequencies as haplogroup definition is based on a nonrandom sampling of single nucleotide polymorphism (i.e., resulting in ascertainment bias with unknown effect on the estimation of diversity and genetic distances).

Isolation by distance

We computed two geographic distance matrices among the sampled populations. The first is the great circle distance, which represents the shortest line between two points and takes into account the curvature of the earth (GEO). The second is the distance in days of walk (DAY), which was computed by one of us (M. T.-P.) by traveling among all groups together with local guides. DAY implicitly reflects the environmental heterogeneities, as it represents the facility to move from one village to another. Pairwise genetic distances at mtDNA (*Fst*) and NRY (*Rst*) were computed using Arlequin 3.5 (Excoffier and Lischer 2010). We refer to them hereafter as Fst_F and Rst_M to highlight that *Fst* was computed in females (from mtDNA) and *Rst* in males (from NRY). The correlations

Figure 1. Geographic map of West New Guinea with the approximate location of the studied populations. *A*: Asmat; *C*: Citak; *D*: Dani; *K*: Ketengban; *M*: Mappi; *U*: Una; *W*: Awyu; *Y*: Muyu.

among the four matrices were estimated by pairwise Mantel tests, with the significance assessed after 10,000 permutations. Isolation by distance was further tested at both genetic markers by means of the Mantel correlogram (Legendre and Fortin 1989) using GEO or DAY as a geographic distance matrix. The number of classes was determined using Surge's rule and significance within each class was assessed after 1000 permutations. All these analyses were performed using the libraries *ecodist* and *gdistance* implemented in the R statistical package (R Development Core Team 2011).

Indirect inferences on *Nm* values in a metapopulation

Human populations are almost never completely isolated but, rather, they belong to a metapopulation of demes exchanging migrants at various rates and with various dispersal kernels. The gene genealogy relating a sample of lineages extracted from a deme belonging to a metapopulation, as well as that of a pool of lineages taken from different demes, is mostly determined by the product of the effective population size *N* and the migration rate *m* (Wakeley 1999, 2001; Ray et al. 2003; Stadler et al. 2009). Contrasting the shape of the genealogy at various sampling level (i.e., single deme vs. a pool of lineages from different demes) provides indirect information on the absolute *Nm* value (Stadler et al. 2009) independently of the knowledge of the mutation rate *μ*. The idea behind this approach is that in species experiencing range expansion (or more generally organized in a large array of subpopulations or demes) the coalescent history of a sample of lineages can be divided into a *scattering* and a *collecting* phase (Wakeley 1998, 1999). The relative length of the two phases determines the shape of the gene genealogy and it mostly depends on *Nm* (Wakeley 1999; Ray et al. 2003). This holds true for lineages sampled within a deme, scattered throughout the range of the species or pooled from various demes (Stadler et al. 2009). Contrasting the shape of a gene genealogy in a metapopulation at all these sampling intensities can therefore provide information on *Nm*. High *Nm* values will determine signature of population growth at all sampling levels (Stadler et al. 2009). For decreasing *Nm*, the signature of the range expansion will be lost first when sampling lineages from a single deme, then when pooling several lineages coming from different demes. The higher the number of lineages per deme pooled, the faster the signature of expansion will be lost. A scattered sample, where each lineage is extracted from a different deme, will be the last to lose such signature (Wakeley 1999). Investigating the shape of the gene genealogy at various sampling levels is preferable to the comparison of fixation indices such as

Fst (Excoffier et al. 1992) and *Rst* (Slatkin 1995), commonly used to estimate *Nm*. These fixation indices are dependent on μ and on the molecular evolutionary characteristic of the markers under examination (Hedrick 2005). Moreover, they are based on simplifying assumptions which do not always hold in real settings (Whitlock and McCauley 1999), while metapopulation and sampling theory is robust to various population genetic models (Wakeley 1999, 2004; Ray et al. 2003; Wilkins 2004; Stadler et al. 2009).

To determine the shape of the genealogy, we used a Bayesian-based coalescent approach and compared different demographic models by means of Bayes Factors (BF). We used BEAST (Drummond et al. 2012) to contrast a constant size model versus the extended Bayesian skyline plot (Heled and Drummond 2008) for mtDNA, and Batwing (Wilson et al. 2003) to contrast a constant size model versus a constant population starting an expansion T generations before present for NRY. Default priors were used in BEAST, whereas priors as in Mona et al. (2007) were set in Batwing. We ran all datasets with both software for 100,000,000 iterations with a 10% burn-in and a thinning of 1000. Convergence was checked by running each dataset twice and by reaching an effective sample size higher than 200 for all parameters in each analysis. Marginal likelihood was evaluated using the harmonic mean estimator (Kass and Raftery 1995). BF were computed as twice the difference of the natural logarithm of the marginal likelihoods and interpreted using the Jeffrey scale as reported in Kass and Raftery (1995). The harmonic mean is a simple estimator of the marginal likelihood and some concerns have recently emerged on its performance (Baele et al. 2012). The advantage of using the harmonic mean is its computational efficiency, which is important because we run a large number of model comparison analyses. The analyses were performed in: (i) each of the eight groups; (ii) the total pooled sample; (iii) 100 datasets of (a) 16 lineages obtained by resampling two lineages per village (group 2L); (b) 24 lineages obtained by resampling three lineages per village (group 3L); (c) 32 lineages obtained by resampling four lineages per village (group 4L). In total, we analyzed 309 datasets under two different models for the two markers, amounting to 1236 coalescent analyses. The reasoning behind resampling 100 times two, three, or four lineages per village was to obtain a BF distribution at each sampling intensity to assess the impact of stochastic variance in the coalescent process.

Spatial explicit simulations

We performed a set of spatial explicit simulations of the demographic history of males and females in WNG using the software SPLATCHE (Currat et al. 2004). SPLATCHE allows the simulation of a range expansion of haploid individuals over a two-dimensional array of demes arranged on a lattice and exchanging migrants with their four nearest neighbors. Simulations are done in two consecutive steps, namely the forward (demographic) and the backward (coalescent) steps. The forward simulation starts from an ancestral deme, which sends migrants to its neighboring demes. Migrations to empty demes represent new colonization events. Each deme has an intrinsic growth rate *g* and its density is logistically regulated by its carrying capacity (*N*) (Ray et al. 2003). SPLATCHE uses a map of *N* values which can be also changed at user-defined time points. In this way, it is possible to model both spatial and temporal heterogeneity, by varying habitat quality (the *N* values) in space and time. After the regulation step, migrants are sent to the four neighboring demes at rate *m*. The process is repeated for successive generations for each nonempty deme, resulting in a wave of advance of the whole population. At equilibrium, each deme will send *Nm* migrants per generation to its surrounding demes. At each generation, the demographic and migration histories of every deme are stored in a database, which is then used in the backward coalescent step. The second phase of the algorithm then starts at the present generation, proceeding backward in time. The effective number of individuals present in a deme is used to compute the probability of a coalescent event, and the migration rates determine the probability of each sampled gene to emigrate, backwards in time, to the surrounding demes. The coalescent process stops after all genes have coalesced.

Spatial simulations were used to investigate under which demographic conditions we could reproduce the Rst_M/Fst_F ratio observed in our data. Three of eight populations practice agriculture (AG groups), whereas the remaining five are hunter/fisher–gatherers (HG groups). Differences in *Nm* values between males (Nm_M) and females (Nm_F) can be due (among other factors) to different marital residence pattern and variance in reproductive success (e.g., due to polygyny). It is not known when these cultural behaviors arose in human populations and if they differ markedly between AG and HG groups (Marlowe 2004). For this reason, we devised six evolutionary scenarios and tested a number of demographic parameters under each of them, considering also the possible increase in the carrying capacity of AG due to agriculture. The six scenarios are listed in Table 1: (i) *Scenario 1*: differences between Nm_M and Nm_F in HG, but not in AG. Postagriculture demographic expansion in AG; (ii) *Scenario 2*: differences between Nm_M and Nm_F in AG, but not in HG. Postagriculture demographic expansion in AG; (iii) *Scenario 3*: reduction in Nm_M compared with Nm_F in both

Table 1. The evolutionary scenario tested.

Model	Nm HG	Nm AG	Agriculture[1]	Description
1	$Nm_M \neq Nm_F$	$Nm_M = Nm_F$	Yes	Sex differences in HG but not in AG. Increased carrying capacity in AG due to agriculture.
2	$Nm_M = Nm_F$	$Nm_M \neq Nm_F$	Yes	Sex differences in AG but not in HG. Increased carrying capacity in AG due to agriculture.
3	$Nm_M < Nm_F$	$Nm_M < Nm_F$	Yes	Sex differences in both AG and HG. Increased carrying capacity in AG due to agriculture.
4	$Nm_M \neq Nm_F$	$Nm_M \neq Nm_F$	No	Sex differences in both AG and HG. No effect of agriculture
5	$Nm_M < Nm_F$[2]	$Nm_M < Nm_F$	Yes	Sex differences in both AG and HG. These differences appeared only after the beginning of agriculture. Increased carrying capacity in AG due to agriculture
6	$Nm_M < Nm_F$[2]	$Nm_M = Nm_F$	Yes	Sex differences in HG. These differences appeared only after the beginning of agriculture. Increased carrying capacity in AG due to agriculture

We assumed agriculture started 8000 years B.P. Before agriculture, there is no difference in Nm between AG and HG.

[1]Agriculture increased ("Yes") or not ("No") the carrying capacity in AG, but not in HG.

[2]Difference between Nm_M and Nm_F begins only after the emergence of agriculture.

AG and HG. Postagriculture demographic expansion in AG; (iv) *Scenario 4*: differences between Nm_M and Nm_F in both AG and HG. No postagriculture demographic expansion in AG; (v) *Scenario 5*: reduction in Nm_M compared with Nm_F in both AG and HG. These differences arose in all demes only after the emergence of agriculture. Postagriculture demographic expansion in AG; (vi) *Scenario 6*: reduction in Nm_M compared with Nm_F in HG. These differences arose in HG only after the emergence of agriculture. Postagriculture demographic expansion in AG.

We set the beginning of the range expansion into New Guinea at 2000 generations ago, which roughly corresponds to the first human presence in the interior highlands at 49,000 years b.p. (Summerhayes et al. 2010) assuming a generation time of 25 years (Fenner 2005). For simplicity and because of the lack of data specific to New Guinea, we assumed the same generation time for males and females even though Fenner (2005) suggested the value of 31 and 25, respectively, for ancient populations. For all scenarios and all demographic parameters, we first modeled a rapid colonization of the whole of WNG in approximately 100 generations and changed the Nm thereafter. This choice was made for two reasons: first, to ensure the same colonization time for both sexes, and second, to cope with the earliest human remains in Australia. Human remains are as old as 46,000 years b.p. (Hudjashov et al. 2007), implying that the wave of advance through New Guinea must have been fast. We assumed the origin of the range expansion in the Bird's Head region (North West of New Guinea) as it was proposed to be one of the possible arrival areas of modern humans (Birdsell 1977). We also ran a set of simulations placing the origin of the expansion in the southern region of West New Guinea, obtaining similar results. To calibrate N values, we used density data available from modern and ancient hunter–gatherers group (Steele et al. 1998; Bocquet-Appel and Demars 2000; Binford 2001). By fixing the carrying capacity of HG groups to 40 (Currat

and Excoffier 2004), we varied the total number of demes of WNG in order to obtain a density of 0.16, 0.34, and 1 per square kilometer. These densities refer to the population size before agriculture, when all demes had the same carrying capacity (no difference between HG and AG groups). The value of 1 has been used as an upper bound as it exceeds the density range proposed for hunter–gatherer groups (Binford 2001). All results presented are based on a density of 0.16, but no significant differences were obtained in the other two cases. Briefly, a density of 0.16 corresponds to 448 demes and a total effective male or female size of 17,920 (leading to a total number of inhabitants of 17,920 × 4 = 71,680 following the computation of Currat and Excoffier [2004]). Altitudinal values were used to approximately define the number of AG demes (as agriculture is mostly practiced in the interior highlands), which we set to 90 for the 0.16 density map. The effect of agriculture (scenarios 1, 2, 3, 5, and 6) was simulated by suddenly increasing the carrying capacity of AG demes at 8000 years b.p. (Denham et al. 2003; Denham 2005). The migration rates m were set to obtain an Nm_M and Nm_F ranging from 0.6 to 20 for HG and from 10 to 150 for AG (in scenarios involving an effect of agriculture). Mutation rate for the hypervariable region of mtDNA was set according to Soares et al. (2009), whereas for NRY we used an average value of 0.002 per generation per locus, according to the median posterior distribution obtained after the runs in Batwing. We simulated genetic data from eight demes with the sample size and coordinate position of our eight populations (therefore, three AG and five HG groups). For each parameter combination under each scenario we performed 1000 coalescent simulations. Fst_F and Rst_M were computed with Arlsumstat (Excoffier and Lischer 2010) and the averages were visualized by means of a contour plot. The maps corresponding to the three densities used are available upon request as raster map which can be imported in R using the *adehabitat* library.

Results

Despite being highly and significantly correlated (Table 2), DAY and GEO matrices behave rather differently when compared with both Rst_M and Fst_F pairwise distances. DAY is a good predictor of Rst_M matrix (0.693, $P < 0.05$), but not of Fst_F (Table 2). Moreover, the Mantel correlogram shows also a different pattern between the two markers, even though we note that the apparent clinal distribution of the NRY variation is mainly driven by the outlier Dani population (Fig. 2). Indeed, the correlation between DAY and Rst_M drop to 0.38 when excluding the Dani ($P \approx 0.20$). Conversely, GEO is not correlated with any of the two genetic distance matrices (Table 2) and shows no

clear trend when used in the Mantel correlogram analysis (Fig. 2).

We computed the BF contrasting a constant size model versus the extended Bayesian skyline plot in the mtDNA dataset. None of the populations except Dani and Ketengban showed any support for one of the two models (Table 3). The pooled sample was no exception, with a BF of 0.49 in favor of the skyline model (Table 3). However, a qualitative comparison of the reconstructed variation in *Ne* through time highlights some differences between the single populations and the pooled sample (Figs. 3 and S1). Although each of the single populations displays a modest and recent signature of population expansion, the pooled sample experienced a strong demographic growth starting around 50 kya before present (assuming the mutation rate as in Soares et al. [2009]). This growth is well supported by the credible interval (Fig. 3) and coincides approximately with the arrival time of modern humans in New Guinea (Summerhayes et al. 2010). We computed BF contrasting a constant size model versus an expansion model in the NRY dataset. According to the scale of Jeffrey, we found very strong evidence in favor of a constant population size model in all populations and particularly in the pooled sample (Table 3). We also reported the median and 95% credible interval of the *Ne* for all populations for both markers (Table 3). AG groups have lower NRY *Ne* compared with

Table 2. Pairwise Mantel correlation matrix.

	GEO	DAY	Fst_F	Rst_M
GEO	–	*	n.s.	n.s.
DAY	0.521	–	n.s.	*
Fst_F	0.193	−0.053	–	n.s.
Rst_M	0.225	0.692	0.111	–

GEO, kilometric distance matrix; DAY, walking time distance matrix. Below diagonal: correlation coefficients. Above diagonal: significance of the test after 10,000 permutations. n.s., not significant.
*$P < 0.05$.
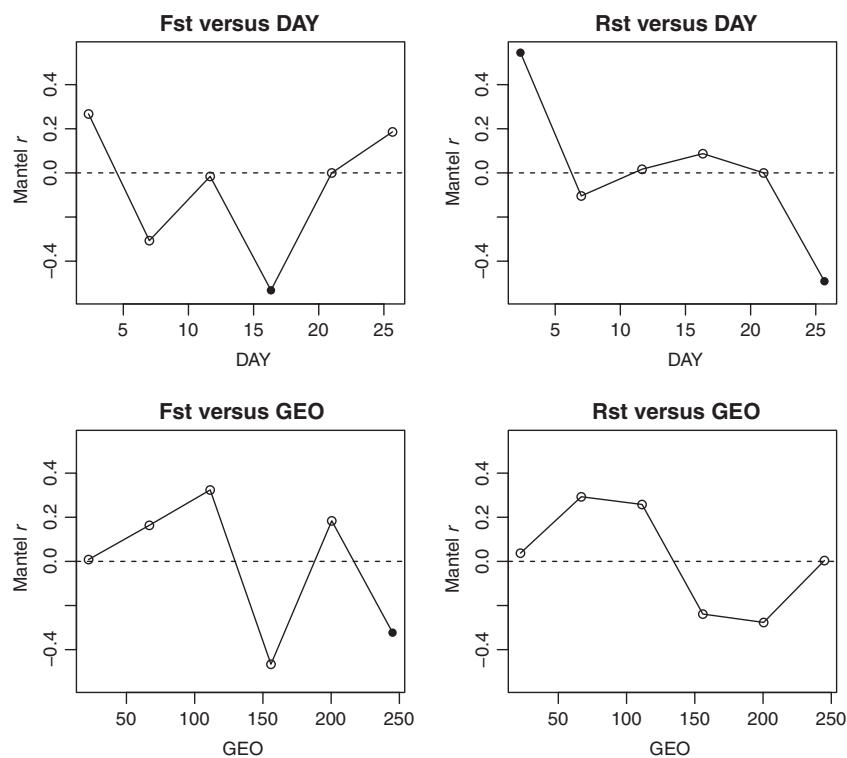
Figure 2. Mantel correlogram. *x-axis*: distance between groups in days of walking (DAY) or kilometers (GEO). *y-axis*: Mantel correlation coefficient. Black dots represent classes with significant correlation coefficient.

Table 3. Coalescent demographic estimate under a constant size model.

Population	mtDNA				NRY			
	n	*k*	*Ne*	BF	*n*	*k*	*Ne*	BF
Asmat	25	17	4218 (1886–6921)	1.43	20	14	609 (160–1050)	71.23***
Awyu	14	11	6461 (2608–11,117)	0.72	10	6	282 (33–628)	27.11***
Citak	39	23	8475 (4610–12,240)	0.12	28	14	473 (130–796)	68.21***
Mappi	19	14	6628 (3214–11,063)	1.77	10	6	631 (114–1224)	51.61***
Muyu	9	8	4770 (1358–9655)	−1.70	6	5	697 (133–1375)	16.49***
Dani	21	17	6529 (3057–10,442)	6.24**	24	7	203 (45–387)	65.35***
Ketengban	23	10	3017 (1306–5098)	2.44*	19	7	165 (24–341)	41.73***
Una	50	28	7119 (4362–10,528)	0.04	46	11	182 (38–328)	90.10***
Pool	200	89	17,298 (10,566–21,242)	0.49	163	56	928 (468–1302)	1156.77***

n, sample size; *k*, number of haplotype; *Ne*, effective population size (in parentheses the 95% high posterior density); BF, Bayes factor. *positive evidence; **strong evidence; ***very strong evidence in favor of one model according to Jeffrey scale. Positive values support the constant model, negative values the skyline. *Ne* values were obtained assuming the mutation rate reported in Soares et al. (2009) for mtDNA and the priors used in Mona et al. (2007) for NRY. Dani, Ketengban, and Una are AG and the other populations are HG.
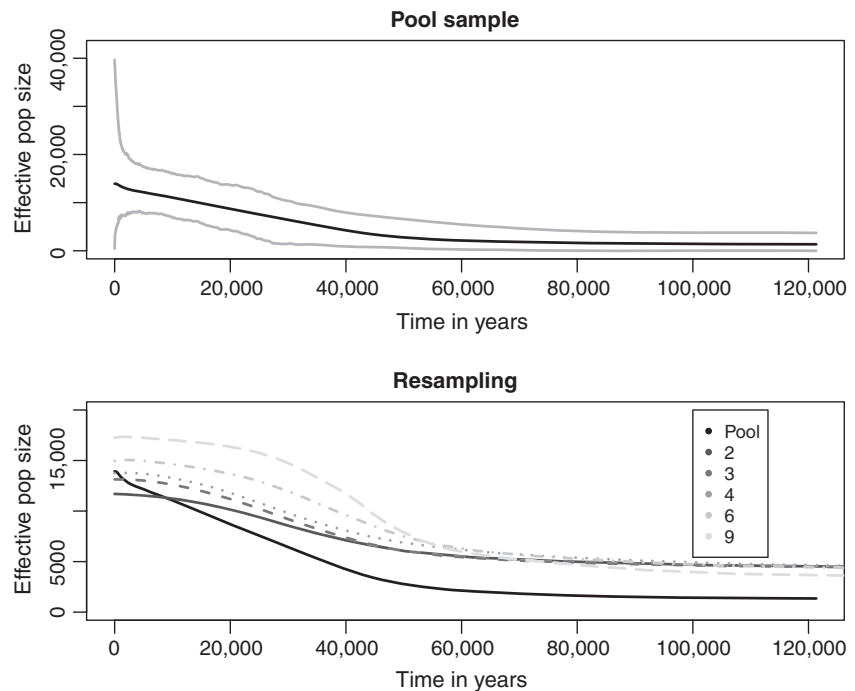
Figure 3. Extended Bayesian skyline plot computed in the: (A) pool sample; (B) Asmat; (C) Una. In (D), we plot the average skyline computed on 100 resampled datasets obtained by pooling 2, 3, 4, 6, or 9 lineages per population. Lines used are: solid, dashed, dotted, dot dash, long dash, or two dashes for the 2, 3, 4, 6, or 9 cases, respectively. *Ne* and coalescent times were scaled assuming the mutation rate reported in Soares et al. (2009).

HG groups, while there is no trend in the mtDNA data (Table 3).

We computed the BF in the resampled dataset and present the results in Table 4. At all sampling intensities, there are approximately the same number of dataset supporting a constant or Bayesian skyline model in mtDNA. Accordingly, the mean BF shows no correlation with the number of lineages sampled per population and in any case supports one of the demographic models tested (Table 4). We also plot the average skyline for all sampling intensities (Fig. 3). In accord with the pooled sample, all skylines support an expansion around 50 Kya,

with a stronger signal for higher sampling intensities (Fig. 3). A completely different picture emerged for the NRY. In the 16 lineages case (group 2L) there are nine datasets supporting an expansion, but only one in the 32 lineages case (group 4L). All the resampled datasets support strongly the constant size model in the 48 lineages case (group 6L) (Table 4). Moreover, there is a positive correlation between the mean BF and the sampling intensities. This result indicates that by increasing the number of lineages per population, the shape of the gene genealogy resembles more what would be expected under constant demography. This means that there will

Table 4. Bayes Factor results on resampled datasets classified according to Jeffrey scale.

Model	Support	mtDNA					Y-chr		
		2L[1]	3L	4L	6L	9L	2L	3L	4L
Constant	Very strong	0	0	0	0	0	0	0	18
	Strong	0	1	0	3	3	46	90	81
	Positive	26	27	36	37	40	36	9	1
Size change	Very strong	0	0	0	0	0	0	0	0
	Strong	0	0	0	3	0	0	1	0
	Positive	14	22	24	28	32	9	0	0
	None	60	50	40	29	25	9	0	0
Mean values		1.23	0.65	0.83	1.23	1.15	19.87	61.78	115.98

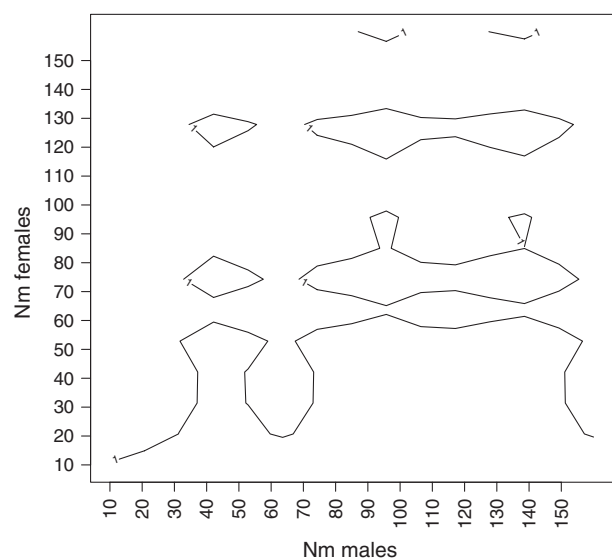In the last row, we reported the mean BF over 100 resampled datasets.
[1]Number of lineages sampled per population.
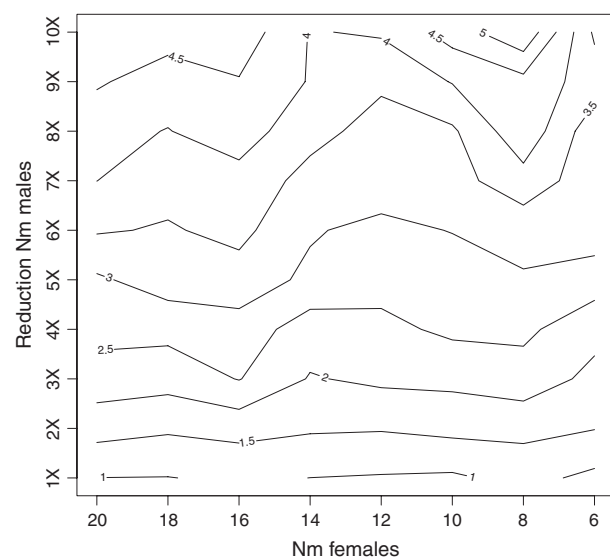
Figure 4. Contour plot obtained under Scenario 1 for *Nm* in AG = 150. *x-axis*: Nm_M of HG. *y-axis*: Nm_F of HG.

Figure 5. Contour plot obtained under Scenario 2 for *Nm* in HG = 1. *x-axis*: Nm_M of AG. *y-axis*: Nm_F of AG.

be more coalescence during the scattering phase, which is what we expect for small *Nm* value. The difference in the shape of the gene genealogy between mtDNA and NRY is therefore consistent with an Nm_M much smaller than Nm_F.

We computed an Rst_M of 0.488 ($P < 0.001$) and an Fst_F of 0.116 ($P < 0.001$) among the sampled populations. The Rst_M/Fst_F ratio is 4.2 which correspond approximately to an Nm_F/Nm_M ratio of 7.26 assuming the Wright (1931) island model. We tested more realistic and complex demographic scenarios by means of spatial explicit simulations. We aimed to determine under each evolutionary scenarios which values of Nm_F and Nm_M could reproduce an Rst_M/Fst_F ratio around 4.2. Contour plots obtained under *Scenario 1* are presented in Figure 4. Under this hypothesis, we varied Nm_M and Nm_F of HG

for fixed *Nm* in AG. We found that only a combination of $Nm_M \approx 1$ (corresponding to an average Rst_M of 0.40 and 0.42 for *Nm* in AG of 150 and 20, respectively) and an Nm_F at least 10 times higher in HG is compatible with observed data, independently from the *Nm* in AG. Generally, reduction in Nm_M must be at least sevenfold larger when compared with Nm_F (Fig. 4 with *Nm* AG of 150; Fig. S2 with *Nm* AG of 20). Similarly, when we assumed that sex-specific differences occurred in HG only after the Neolithic we found still that an Nm_M reduction 10 times higher is needed to generate the observed Rst_M/Fst_F ratio, independently from *Nm* in AG (*Scenario 6*, Figs. 8 and S6). In *Scenario 2*, we tested several combinations of Nm_M and Nm_F of AG for fixed *Nm* in HG. Under this hypothesis, we never found an Rst_M/Fst_F ratio higher than 2 (Fig. 5, *Nm* HG of 1), independently on the *Nm* in HG

(Fig. S3, *Nm* HG of 20). This result suggests that different behavior between males and females in West New Guinea are not (only) related to the emergence of agriculture as they must be present in HG as well in order to obtain such values of Rst_M and Fst_F. *Scenario 3* and *5* assume that differences in the same magnitude between Nm_M and Nm_F are present both in HG and AG. In *Scenario 5,* such differences were established after the emergence of agriculture in all groups, whereas in *Scenario 3* they have
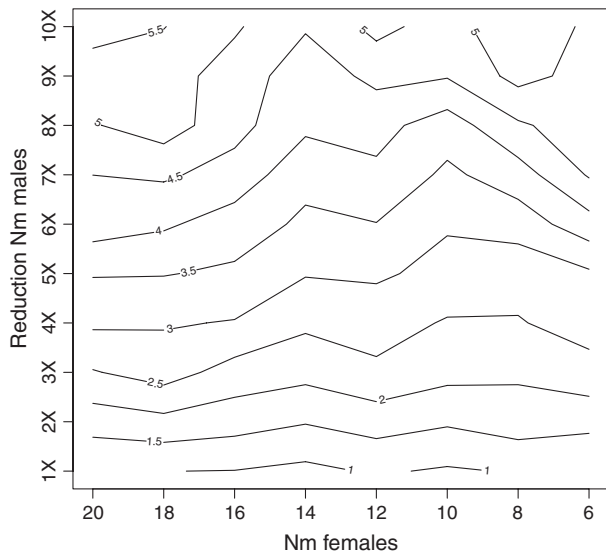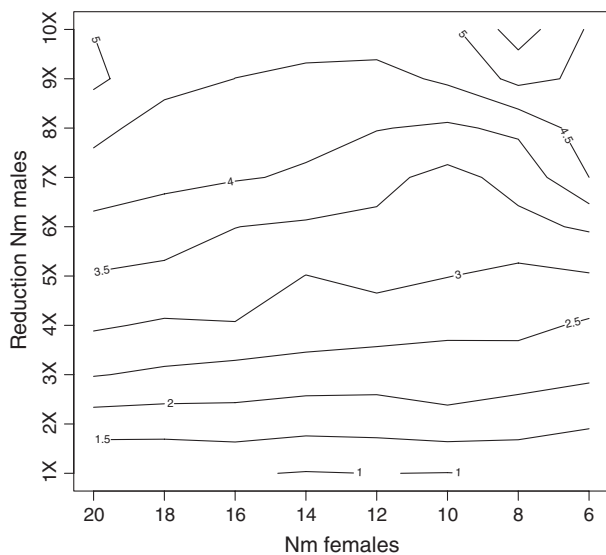
been always present. In Figures 6 and 7, we plot the Rst_M/Fst_F for various Nm_F in HG and an $Nm_F = 150$ in AG for scenario 3 and 5, respectively. In both scenarios, we found that a decrease in Nm_M of at least sixfold is needed to generate an Rst_M/Fst_F ratio higher than 4, independently of the Nm_F set in AG (see Figs. S4 and S5 with $Nm_F = 25$ in AG). Finally, we presented in Fig. 9 the results of *Scenario 4* where we assumed no difference in carrying capacity between HG and AG (i.e., no effect of agriculture). We found a pattern quite similar to *Scenario 1* for various values of *Nm* in AG. However, we note that the absence of a Neolithic expansion increases the Rst_M and Fst_F values rather than their ratio, leading to an average Rst_M of around 0.71 for $Nm_M = 1$. This implies that an $Nm_M \approx 2$ (leading to an average Rst_M of 0.40) and an Nm_F at least seven times higher is more compatible with our data.

Discussion

Uniparental markers, namely mtDNA and NRY, have been used for a long time to characterize the influence of sex-specific behaviors on the genetic structure and diversity of human populations (Heyer et al. 2012). Here, we addressed the general problem of comparing two loci with different mutational dynamics and we showed the benefits of accounting for the environmental features when investigating the spatial distribution of diversity. We used WNG as a case study for several reasons: (i) it is a region with complex environmental features and our samples come from heterogeneous areas; (ii) the eight populations under investigation are patrilocal. Polygyny is widespread too (Heider 1970; Gardner and Weiner 1992; Knauft 1993), although the diffusion of these practices across the whole region is not homogenous and the importance of polygyny in generating sex-specific differences has been recently questioned (Heyer et al. 2012). These characteristics are likely to generate sex-specific genetic patterns; (iii) reduced Y-chromosome but not mtDNA diversity in these populations has been already described (Kayser et al. 2003), but no quantitative test was carried out to characterize male and female metapopulation dynamics.

We first note the importance of computing the real connectivity matrix relating the studied populations. The days of walking required to travel between groups are highly correlated with NRY pairwise distances (Table 2 and Fig. 2), even though it is important to highlight the role played by Dani, which are highly differentiated at NRY, but not at mtDNA and can drive such correlation (which drops to 0.38 and becomes not significant when removing them). At the same time, regardless of the measure of geographic distance used, there is no significant

Figure 6. Contour plot obtained under Scenario 3 for *Nm* in AG = 150. *x-axis*: Nm_F of HG. *y-axis*: reduction intensity of Nm_M in HG and AG.

Figure 7. Contour plot obtained under Scenario 5 for *Nm* in AG = 150. *x-axis*: Nm_F of HG. *y-axis*: reduction intensity of Nm_M in HG and AG.

pattern in the distribution of mtDNA diversity. This finding would have not emerged by using kilometric distances only against which both markers exhibit a similar behavior (Table 2 and Fig. 2). In other words, by overlooking the true connectivity among populations we would have missed the differences in the migration trajectories between males and females. This finding is consistent with patrilocality, where males tend to live in the same village of their parents whereas females follow their husband (Marlowe 2004). Males move following the least costly path according to the environment whereas females more randomly, probably as a consequence of being exchanged.

Not only the direction but also the intensity of gene flow differs between the two sexes. We found an Rst_M/Fst_F ratio of about 4 which equals to a number of migrants per generation (Nm) about seven times higher in females than in males. This value is based on equilibrium model (Wright island model) which also overlooks the molecular properties of the two markers and their effect on the estimation of the fixation indices. To compare Nm between the chosen markers without worrying about their different molecular properties, we investigated the shape of the gene genealogy in all demes and in datasets created by resampling lineages from each of them. Range expansion is still visible in mtDNA, where resampled datasets support a growth around 50,000 years b.p. (Fig. 3), consistent with archaeological records (Summerhayes et al. 2010). Contrary to what we expected from theory (Stadler et al. 2009), we found a stronger expansion for higher sampling intensities. However, the power to detect an expansion using coalescent theory is correlated with the sample size for small datasets (Ramos-Onsins and Rozas 2002). Therefore, the inferred skyline depends both on the true shape of the gene genealogy and the power to correctly recover it. The balance between these two factors also explains why there is no trend in the BF distribution. We found no signature of expansion in the single populations, which suggests that Nm_F must be lower than 20, as simulation studies showed expansions can be detected for $Nm > 20$ (Ray et al. 2003). The picture for the NRY is drastically different, as only a few resampled datasets at the lowest intensity show a gene genealogy consistent with an expansion (Table 4). The signature of the range expansion into WNG has therefore been lost at the male level, which suggests a reduced Nm_M. Even though, the resampling strategy we adopted does not provide a quantitative estimate of the Nm_F/Nm_M ratio, it is an exploratory tool which has several important advantages over other approaches. Not only it can be used to compare different loci but also to get an accurate picture of the metapopulation dynamic. First, it does not rely on gene diversity or Fst, which means that any markers can be compared with and no need to know their evolutionary mechanism or
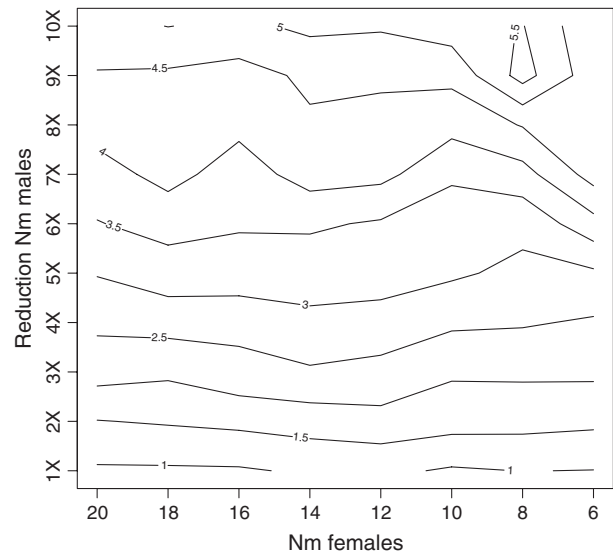
rate. Here, we have analyzed two markers for which a wealth of information about their mutational processes is available from the literature, but we could easily adopt our approach to loci where knowledge is scanty even for humans. Second, it is robust to model misspecification, as it will hold as long as the coalescent process can be divided into a scattering and a collecting phase (which has been shown to work well for many metapopulation models [Wakeley 1999; Ray et al. 2003; Wilkins 2004; De and Durrett 2007]). This can free us from using Fst as an indirect measure of gene flow, as it has been shown that it works poorly under many conditions and even in equilibrium models (Whitlock and McCauley 1999). Third, we got a time estimate of the range expansion occurred in New Guinea which we would have missed by analyzing each population separately only. Finally, we note that estimators of Nm values can be devised exploiting the resampling theory, for example by combining neutrality tests (compound tests) at various sampling intensities and/or using them as new and powerful summary statistics under an approximate bayesian computation inferential procedure. Coalescent approach coupled with sampling theory can be therefore applied to any structured species, provided that it is composed by a large (>100) number of demes.

To further investigate differences between Nm_M and Nm_F we also used spatial explicit simulations. The advantage of using simulations was threefold: first, we explicitly modeled the molecular dynamics of both mtDNA and NRY; second, we accounted for the genetic structure within WNG, including also the unsampled demes; third, we introduced in the population genetic model spatial and temporal heterogeneity (in particular, the effect of agriculture on the carrying capacity). For these reasons, we could not only make quantitative statements about the Nm_F/Nm_M ratio, but also investigate when the differences arose. Independently of the scenario tested, we found that the observed Rst_M/Fst_F ratio is compatible only with a number of male migrants per generation at least six times lower than female migrants (Figs. 4–9). Even though we could not infer precisely when this pattern of migration was established, there are some conclusions we could draw. Differences between male and female pattern must have emerged at least in the Neolithic, not only in AG but also in HG groups (Figs. 4–9). It is possible that, to generate the observed pattern, sex-specific behavior could have emerged even more recently than the Neolithic. However, we did not test for that as it would have increased the number of scenarios to analyze and there are no anthropological hypotheses supporting a more recent shift to patrilocality/polygyny. Many studies have suggested that HG groups are more flexible in terms of postmarital residence pattern, whereas AG groups are
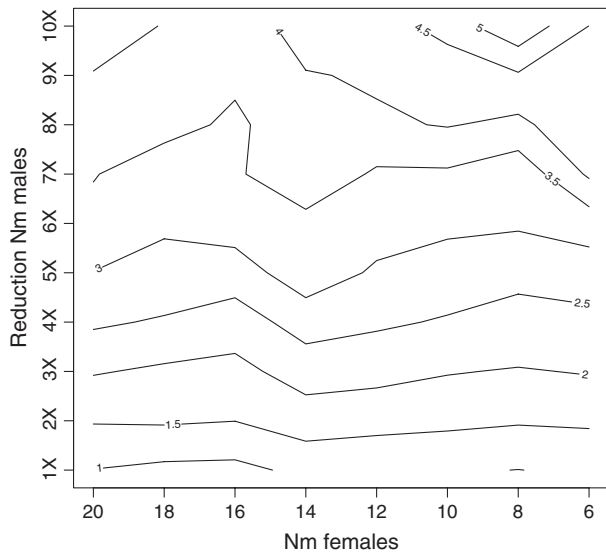
Figure 8. Contour plot obtained under Scenario 6 for *Nm* in AG = 150. *x-axis*: Nm_F of HG. *y-axis*: reduction intensity of Nm_M in HG and AG.

Figure 9. Contour plot obtained under Scenario 4. *x-axis*: Nm_M of AG. *y-axis*: Nm_F of AG.

more predominantly patrilocal (Wilkins and Marlowe 2006). Indeed, in our small dataset with only three AG and five HG populations we found an Nm_F/Nm_M ratio of 14.6 and 1.5 for AG and HG, respectively, under the equilibrium island model. However, considering our more complex simulation framework, we could show that in WNG the differential behavior between males and females in HG is also necessary to generate the observed pattern of differentiation (see Figs. 5 and S3). Moreover, the Rst_M/Fst_F ratio may have originated even assuming no sex-specific behavior in AG groups, provided that either the differences between males and females emerged early in HG groups (Fig. 4) or that they were particularly strong (i.e., Nm_F at least nine times higher than Nm_M, Fig. 9). This result suggests that a key parameter to generate the difference between Rst_M and Fst_F is the number of demes having sex-specific migration pattern in a structured population: if only a small fraction of demes shift to patrilocality and/or polygyny, this will not significantly affect fixation indices. At the same time, if a large fraction of demes shift to patrilocality and/or polygyny, all demes of the metapopulation will be affected. To summarize, it is important to highlight the differences between estimating *Nm* through a spatial explicit model or an equilibrium model. Even if in our case results in terms of Nm_M and Nm_F values are very similar, this may have occurred by chance, as *Fst* is not an accurate estimator of *Nm* (see above). Moreover, we determined by simulations not only a quantitative difference in the number of migrants but also when social behavior started affecting the genetic

variability in West New Guinea. Importantly, we also showed that many but not all populations need to have sex-specific behavior in order to affect the whole metapopulations. As a consequence, even populations with no sex-specific patterns will show differences between Nm_M and Nm_F. Such a fine-scale characterization of metapopulation genetics could have not been possible using equilibrium based methods only.

Here, we have shown how to characterize sex-specific dynamics using both qualitative and quantitative approaches. Even though the specific pattern we observed could have been also influenced by more local events occurred at the single population level (i.e., the Dani and the Ketengban appears to be outlier at the NRY and mtDNA, respectively), the main message of this work is to show the importance of analyzing a structured species under a metapopulation framework and of introducing as much as possible the ecological features of an environment in the population genetics modeling. We did this by both performing spatial and temporal explicit simulations of genetic diversity and by applying indirect metapopulation inferential models. We showed how we can exploit prediction of the metapopulation theory simply by an appropriate sampling of genetic data, gaining a wealth of information (among others, the colonization time of New Guinea and the average connectivity among demes) which we would have missed under more traditional approaches. Moreover, the use of complex simulation schemes gave us the opportunity, not only of directly considering the connectivity among the sampled populations but also of introducing temporal and environmental heterogeneity

and test their effects on genetic diversity. An extension to these analyses would be to implement approximate Bayesian computation (Beaumont et al. 2002) to estimate separately the two parameters for both male and female, and to compare statistically the various demographic scenarios. Unfortunately, spatial explicit simulations are computationally intensive and more independent loci would be required for accurate parameter estimation (Bertorelle et al. 2010). However, their flexibility should prompt them to become a useful tool to investigate a wide range of problem concerning structured populations.

Acknowledgments

We thank Oscar Lao for insightful comments on a previous version of the manuscript. We thank Annabel Whibley for carefully checking the English and for useful comments.

Data Accessibility

All the data used in this work have been previously published in Tommaseo-Ponzetta et al. (2002) and Kayser et al. (2003).

Author Contributions

S. M. and M. T.-P. conceived the project. M. T.-P. travelled among the West New Guinea populations to record the walking distances among them. S. M. and E. M. performed the statistical analyses. S. M. and M. V. wrote the paper.

Conflict of Interest

None declared.

References

Baele, G., P. Lemey, T. Bedford, A. Rambaut, M. A. Suchard, and A. V. Alekseyenko. 2012. Improving the accuracy of demographic and molecular clock model comparison while accommodating phylogenetic uncertainty. Mol. Biol. Evol. 29:2157–2167.

Balaresque, P., F. Manni, J. M. Dugoujon, B. Crousau-Roy, and E. Heyer. 2006. Estimating sex-specific processes in human populations: are XY-homologous markers an effective tool? Heredity (Edinb). 96:214–221.

Beaumont, M. A., W. Zhang, and D. J. Balding. 2002. Approximate Bayesian computation in population genetics. Genetics 162:2025–2035.

Bertorelle, G., A. Benazzo, and S. Mona. 2010. ABC as a flexible framework to estimate demography over space

and time: some cons, many pros. Mol. Ecol. 19:2609–2625.

Binford, L. 2001. Constructing frames of reference. An analytical method for archaeological theory building using hunther-gatherer and environmental data sets. University of California Press, Berkeley.

Birdsell, J. 1977. The recalibration of a paradigm for the first peopling of Greater Australia. Pp. 113–168 in J. Allen, J. Golson, and R. Jones, eds. Sunda and Sahul. Academic Press, London.

Bocquet-Appel, J., and P. Demars. 2000. Population kinetics in the Upper Palaeolithic in Western Europe. J. Archaeol. Sci. 27:551–570.

Currat, M., and L. Excoffier. 2004. Modern humans did not admix with Neanderthals during their range expansion into Europe. PLoS Biol. 2:e421.

Currat, M., N. Ray, and L. Excoffier. 2004. SPLATCHE: a program to simulate genetic diversity taking into account environmental heterogeneity. Mol. Ecol. Notes 4:139–142.

De, A., and R. Durrett. 2007. Stepping-stone spatial structure causes slow decay of linkage disequilibrium and shifts the site frequency spectrum. Genetics 176:969–981.

Delfin, F., S. Myles, Y. Choi, D. Hughes, R. Illek, M. van Oven, et al. 2012. Bridging near and remote Oceania: mtDNA and NRY variation in the Solomon Islands. Mol. Biol. Evol. 29:545–564.

Denham, T. P. 2005. Agricultural origins and the emergence of rectilinear ditch networks in the Highlands of New Guinea. Pp. 329–361 in A. Pawley, R. Attenborough, J. Golson, and R. Hide, eds. Papuan pasts: cultural, linguistic and biological histories of Papuan speaking peoples. Pacific Linguistics, Canberra.

Denham, T. P., S. G. Haberle, C. Lentfer, R. Fullagar, J. Field, M. Therin, et al. 2003. Origins of agriculture at Kuk Swamp in the highlands of New Guinea. Science 301:189–193.

Drummond, A. J., M. A. Suchard, D. Xie, and A. Rambaut. 2012. Bayesian phylogenetics with BEAUti and the BEAST 1.7. Mol. Biol. Evol. 29:1969–1973.

Excoffier, L., and H. E. Lischer. 2010. Arlequin suite ver 3.5: a new series of programs to perform population genetics analyses under Linux and Windows. Mol. Ecol. Resour. 10:564–567.

Excoffier, L., P. E. Smouse, and J. M. Quattro. 1992. Analysis of molecular variance inferred from metric distances among DNA haplotypes: application to human mitochondrial DNA restriction data. Genetics 131:479–491.

Felsenstein, J. 2006. Accuracy of coalescent likelihood estimates: do we need more sites, more sequences, or more loci? Mol. Biol. Evol. 23:691–700.

Fenner, J. N. 2005. Cross-cultural estimation of the human generation interval for use in genetics-based population divergence studies. Am. J. Phys. Anthropol. 128:415–423.

Fullagar, R., D. Price, and L. Head. 1996. Early human occupation of northern Australia: archaeology and

thermoluminescence dating of Jinmium rock-shelter, Northern Territory. Antiquity 70:751–773.

Fuselli, S., E. Tarazona-Santos, I. Dupanloup, A. Soto, D. Luiselli, and D. Pettener. 2003. Mitochondrial DNA diversity in South America and the genetic history of Andean highlanders. Mol. Biol. Evol. 20:1682–1691.

Gardner, D., and J. Weiner. 1992. Social anthropology in Papua New Guinea. Pp. 119–135 *in* R. Attenborough and M. Alpers, eds. Human biology in Papua New Guinea: the small cosmos. Clarendon Press, Oxford.

Golson, J. 1990. Kuk and the development of agriculture in New Guinea retrospection and introspection. Pp. 139–147 *in* D. Yen and J. Mummery, eds. Pacific production systems: approaches to economic prehistory. Australian National University, Canberra.

Gunnarsdottir, E. D., M. R. Nandineni, M. Li, S. Myles, D. Gil, B. Pakendorf, et al. 2012. Larger mitochondrial DNA than Y-chromosome differences between matrilocal and patrilocal groups from Sumatra. Nat. Commun. 2:228.

Hedrick, P. W. 2005. A standardized genetic differentiation measure. Evolution 59:1633–1638.

Heider, K. 1970. The Dugum Dani: a Papuan Culture in the Highlands of West New Guinea. Aldine Publishing, Chicago, IL.

Heled, J., and A. J. Drummond. 2008. Bayesian inference of population size history from multiple loci. BMC Evol. Biol. 8:289.

Heyer, E., R. Chaix, S. Pavard, and F. Austerlitz. 2012. Sex-specific demographic behaviours that shape human genomic variation. Mol. Ecol. 21:597–612.

Hudjashov, G., T. Kivisild, P. A. Underhill, P. Endicott, J. J. Sanchez, A. A. Lin, et al. 2007. Revealing the prehistoric settlement of Australia by Y chromosome and mtDNA analysis. Proc. Natl Acad. Sci. USA 104:8726–8730.

Hudson, R. 1990. Gene genealogies and the coalescent process. Pp. 1–44 *in* D. Futuyma and J. Antonovics, eds. Oxford surveys in evolutionary biology. Oxford University Press, New York.

Kass, R., and A. Raftery. 1995. Bayes Factors. J. Am. Stat. Assoc. 90:773–795.

Kayser, M., S. Brauer, G. Weiss, W. Schiefenhovel, P. Underhill, P. Shen, et al. 2003. Reduced Y-chromosome, but not mitochondrial DNA, diversity in human populations from West New Guinea. Am. J. Hum. Genet. 72:281–302.

Kemp, B. M., A. Gonzalez-Oliver, R. S. Malhi, C. Monroe, K. B. Schroeder, J. McDonough, et al. 2012. Evaluating the Farming/Language Dispersal Hypothesis with genetic variation exhibited by populations in the Southwest and Mesoamerica. Proc. Natl Acad. Sci. USA 107:6759–6764.

Knauft, B. 1993. South Coast New Guinea Cultures. History, comparison, dialectic. Cambridge University Press, Cambridge.

Legendre, P., and M. Fortin. 1989. Spatial pattern and ecological analysis. Vegetatio 80:107–138.

Marlowe, F. W. 2004. Marital residence among foragers. Curr. Anthropol. 45:277–284.

McRae, B. H., and P. Beier. 2007. Circuit theory predicts gene flow in plant and animal populations. Proc. Natl Acad. Sci. USA 104:19885–19890.

Meirmans, P. G. 2006. Using the AMOVA framework to estimate a standardized genetic differentiation measure. Evolution 60:2399–2402.

Metzker, M. L. 2010. Sequencing technologies – the next generation. Nat. Rev. Genet. 11:31–46.

Mona, S., M. Tommaseo-Ponzetta, S. Brauer, H. Sudoyo, S. Marzuki, and M. Kayser. 2007. Patterns of Y-chromosome diversity intersect with the Trans-New Guinea hypothesis. Mol. Biol. Evol. 24:2546–2555.

Nasidze, I., E. Y. Ling, D. Quinque, I. Dupanloup, R. Cordaux, S. Rychkov, et al. 2004. Mitochondrial DNA and Y-chromosome variation in the caucasus. Ann. Hum. Genet. 68:205–221.

O'Connell, J., and J. Allen. 1998. When did humans first arrive in Greater Australia and why is it important to know? Evol. Anthropol. 6:132–146.

Oota, H., W. Settheetham-Ishida, D. Tiwawech, T. Ishida, and M. Stoneking. 2001. Human mtDNA and Y-chromosome variation is correlated with matrilocal versus patrilocal residence. Nat. Genet. 29:20–21.

R Development Core Team. 2011. R: a language and environment for statistical computing. R Foundation for Statistical Computing, Vienna, Austria. ISBN 3-900051-07-0. Avalable at http://www.R-project.org/.

Ramos-Onsins, S. E., and J. Rozas. 2002. Statistical properties of new neutrality tests against population growth. Mol. Biol. Evol. 19:2092–2100.

Ray, N., M. Currat, and L. Excoffier. 2003. Intra-deme molecular diversity in spatially expanding populations. Mol. Biol. Evol. 20:76–86.

Roberts, R., R. Jones, and M. Smith. 1990. Thermoluminescence dating of a 50,000-year-old human occupation site in northern Australia. Nature 345:153–156.

Segurel, L., B. Martinez-Cruz, L. Quintana-Murci, P. Balaresque, M. Georges, T. Hegay, et al. 2008. Sex-specific genetic structure and social organization in Central Asia: insights from a multi-locus study. PLoS Genet. 4:e1000200.

Seielstad, M. T., E. Minch, and L. L. Cavalli-Sforza. 1998. Genetic evidence for a higher female migration rate in humans. Nat. Genet. 20:278–280.

Slatkin, M. 1995. A measure of population subdivision based on microsatellite allele frequencies. Genetics 139:457–462.

Soares, P., L. Ermini, N. Thomson, M. Mormina, T. Rito, A. Rohl, et al. 2009. Correcting for purifying selection: an improved human mitochondrial molecular clock. Am. J. Hum. Genet. 84:740–759.

Stadler, T., B. Haubold, C. Merino, W. Stephan, and P. Pfaffelhuber. 2009. The impact of sampling schemes on the

site frequency spectrum in nonequilibrium subdivided populations. Genetics 182:205–216.

Steele, J., J. Adams, and T. Sluckin. 1998. Modelling Paleoindian dispersals. World Archaeol. 30:286–305.

Summerhayes, G. R., M. Leavesley, A. Fairbairn, H. Mandui, J. Field, A. Ford, et al. 2010. Human adaptation and plant use in highland New Guinea 49,000 to 44,000 years ago. Science 330:78–81.

Thorne, A., R. Grun, G. Mortimer, N. A. Spooner, J. J. Simpson, M. McCulloch, et al. 1999. Australia's oldest human remains: age of the Lake Mungo 3 skeleton. J. Hum. Evol. 36:591–612.

Tommaseo-Ponzetta, M., M. Attimonelli, M. De Robertis, F. Tanzariello, and C. Saccone. 2002. Mitochondrial DNA variability of West New Guinea populations. Am. J. Phys. Anthropol. 117:49–67.

Wakeley, J. 1998. Segregating sites in Wright's island model. Theor. Popul. Biol. 53:166–174.

Wakeley, J. 1999. Nonequilibrium migration in human history. Genetics 153:1863–1871.

Wakeley, J. 2001. The coalescent in an island model of population subdivision with variation among demes. Theor. Popul. Biol. 59:133–144.

Wakeley, J. 2004. Metapopulation models for historical inference. Mol. Ecol. 13:865–875.

Wakeley, J. 2008. Coalescent Theory: an Introduction. Roberts & Company, Greenwood Village, Colorado.

Wakeley, J., and S. Lessard. 2003. Theory of the effects of population structure and sampling on patterns of linkage disequilibrium applied to genomic data from humans. Genetics 164:1043–1053.

Whitlock, M. C., and D. E. McCauley. 1999. Indirect measures of gene flow and migration: FST not equal to 1/(4Nm + 1). Heredity 82(Pt 2):117–125.

Wilder, J. A., S. B. Kingan, Z. Mobasher, M. M. Pilkington, and M. F. Hammer. 2004. Global patterns of human mitochondrial DNA and Y-chromosome structure are not influenced by higher migration rates of females versus males. Nat. Genet. 36:1122–1125.

Wilkins, J. F. 2004. A separation-of-timescales approach to the coalescent in a continuous population. Genetics 168:2227–2244.

Wilkins, J. F., and F. W. Marlowe. 2006. Sex-biased migration in humans: what should we expect from genetic data? BioEssays 28:290–300.

Wilson, I. J., M. Weale, and D. J. Balding. 2003. Inferences from DNA data: population histories, evolutionary processes and forensic match probabilities. J. R. Stat. Soc. Ser. A 166:155–188.

Wood, E. T., D. A. Stover, C. Ehret, G. Destro-Bisol, G. Spedini, H. McLeod, et al. 2005. Contrasting patterns of Y chromosome and mtDNA variation in Africa: evidence for sex-biased demographic processes. Eur. J. Hum. Genet. 13:867–876.

Wright, S. 1931. Evolution in Mendelian Populations. Genetics 16:97–159.

Supporting Information

Additional Supporting Information may be found in the online version of this article:

Figure S1. Extended Bayesian skyline plot computed in the each population. *Ne* and coalescent times were scaled assuming the mutation rate reported in Soares et al. (2009).

Figure S2. Contour plot obtained under Scenario 1 for Nm in AG = 20. *x-axis*: Nm_M of HG. *y-axis*: Nm_F of HG.

Figure S3. Contour plot obtained under Scenario 2 for Nm in HG = 20. *x-axis*: Nm_M of AG. *y-axis*: Nm_F of AG.

Figure S4. Contour plot obtained under Scenario 3 for Nm in AG = 25. *x-axis*: Nm_F of HG. *y-axis*: reduction intensity of Nm_M in HG and AG.

Figure S5. Contour plot obtained under Scenario 5 for Nm in AG = 25. *x-axis*: Nm_F of HG. *y-axis*: reduction intensity of Nm_M in HG and AG.

Figure S6. Contour plot obtained under Scenario 6 for Nm in AG = 25. *x-axis*: Nm_F of HG. *y-axis*: reduction intensity of Nm_M in HG and AG.